A Stable Radical Anion of Quinoxalin-2(1*H*)-one in Aerial Dioxygen Activation under Wet-Condition

Sudip Sau,† Sathi Sahoo,† Anupam Manna, and Prasenjit Mal*

School of Chemical Sciences, National Institute of Science Education and Research (NISER), An OCC of Homi Bhaba National Institute, Bhubaneswar, PO Bhimpur-Padanpur, Via Jatni, District Khurda, Odisha 752050, India.

E-mail: pmal@niser.ac.in

† Equal contributing authors

GRAPHICAL ABSTRACT

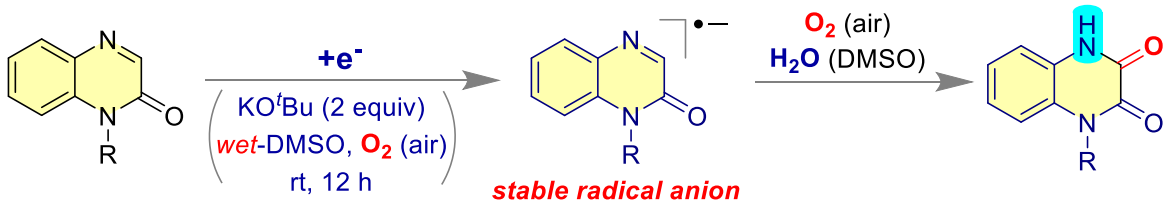

ABSTRACT

In this report, we describe a highly convenient, non-photochemical and unprecedented method for generating stable radical anions and activating atmospheric dioxygen in wet environments. This activation occurs in aerobic and ambient reaction conditions, specifically in the context of quinoxalin-2(*1*H)-one oxygenation, with KO^{t}Bu. The outcome is the successful demonstration of a straightforward method for synthesizing quinoxaline-2,3-dione. Notably, the crucial role of KO^{t}Bu as a single electron transfer (SET) reagent is emphasized, as it initiates dioxygen activation, thereby triggering the oxygenation reaction.

KEYWORDS. Aerial Dioxygen Activation; Oxygenation of Heterocycles; Potassium *tert*-Butoxide; Single Electron Transfer; Stable Radical Anion; Quinoxalin-2(1*H*)-one

INTRODUCTION

The stabilization of reactive organic radicals and radical anions through rational design is crucial for their applications in spin-related fields such as organic electronics,[1] magnets,[2] catalysis,[3] etc.[4] These inherently transient radicals or radical anions are challenging to capture and extremely difficult to utilize in chemical reactions.[5] Nevertheless, radical anions are recognized for their application as visible light photocatalysts.[3, 6] Various strategies for the stabilization of radical anion involve electron delocalization in molecular design,[7] steric hindrance with bulky groups,[8] incorporation into stable frameworks,[9] and electronic structure modification.[10-12] Despite these efforts, creating stable radical anions suitable for ambient chemical reactions remains challenging due to reactivity and susceptibility to environmental factors like air and moisture.[13] The ketyl radical - a stable radical anion, that is formed from the reaction of sodium and benzophenone, serves as a widely used desiccant in laboratory settings.[14] Ketyls exhibit rapid reactivity with water, peroxides, and oxygen. Therefore, the appearance of a deep purple coloration serves as a qualitative indicator of dryness, absence of peroxides, and oxygen-free conditions in the environment.

Molecular oxygen ($^3O_2$) is a paramagnetic diatomic molecule with a ground state spin value of S=1. It's widely present, stable, and abundant. With significance in various atmospheric, chemical, and biological processes, it constitutes about one-fifth of the atmosphere. This makes it an economical, eco-friendly, and atom-efficient oxygenation source.[15] The activation of $^3O_2$ plays a critical role in diverse fields, spanning from biology to materials chemistry.[16-17] Transforming $^3O_2$ into the reactive oxygen species like $^1O_2$, $O_2^{\bullet-}$, $^{\bullet}OH$, H_2O_2, which serve as potent oxidants, stands as an effective approach to initiate desired oxidation reactions. This approach finds extensive use in both environmental and organic contexts.[18]

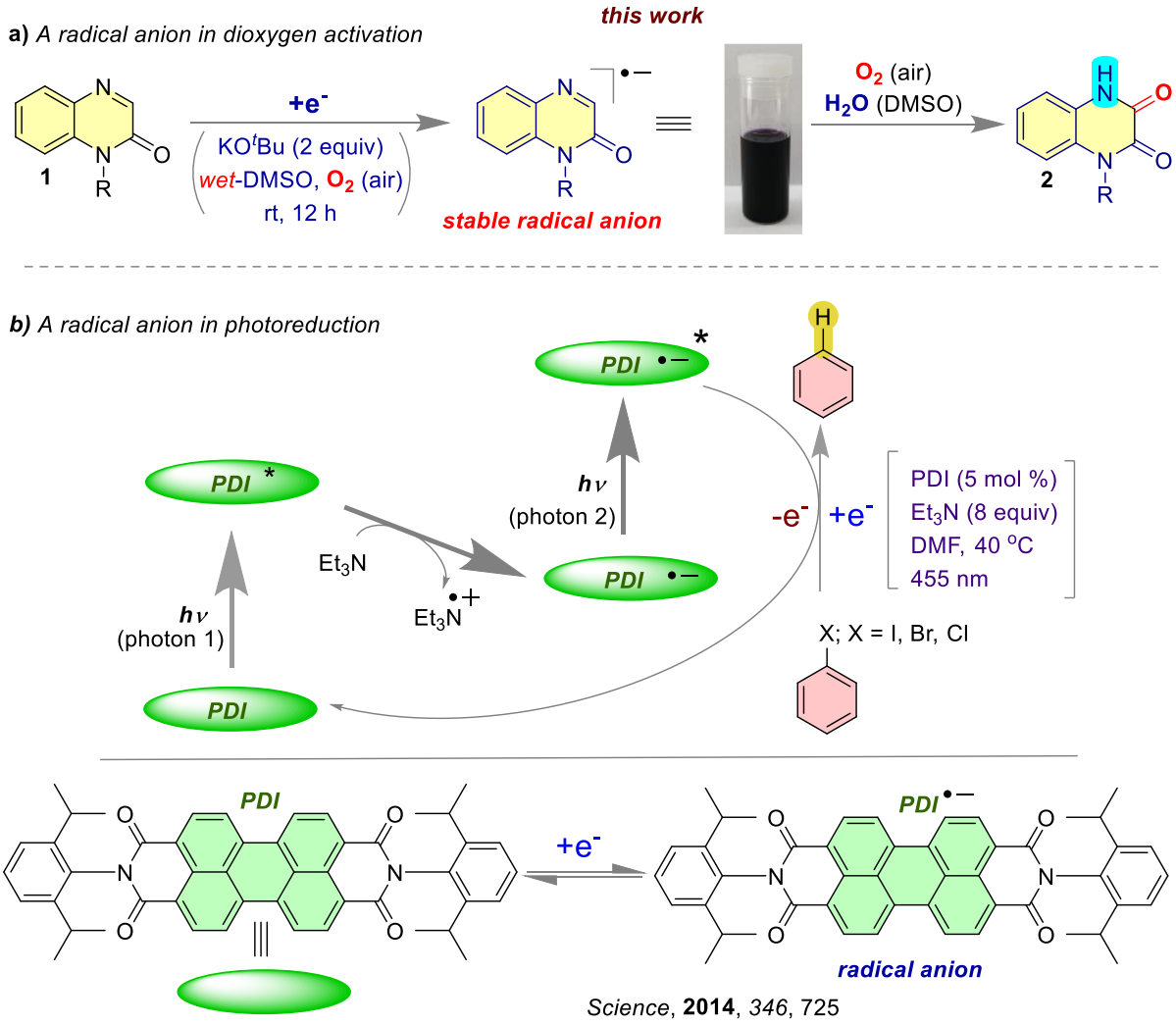

Figure 1. a) A non-photochemical and unprecedented approach to generate stable radical anions and utilize them for activating atmospheric dioxygen under a wet-environment. b) Photochemically generated radical anions *via* two-photon absorption, and their subsequent photoreduction.[6]

Molecular oxygen activation has been extensively documented in the literature through biological, chemical, and photocatalytic pathways.[19-20] However, our study explores the ambient-generation of radical anion intermediates to activate oxygen. Specifically, it targets the oxygenation of quinoxalin-2(*1*H)-ones using O_2 (Figure 1a) using an electron transfer agent potassium tertiary butoxide (KO^{t}Bu).[21] Notably, the activation of molecular oxygen through

the generation of a stable radical anion intermediates *in situ*, under ambient and wet reaction conditions, remains a largely unexplored avenue. Moreover, the available oxygenation methods often rely on expensive transition-metal catalysts.[22-24] Thus, the quest for eco-friendly, cost-effective protocols in synthetic organic chemistry gains significance.[25-27]

König and his co-workers demonstrated a *Z*-scheme (Figure 1b),[6] resembling biological photosynthesis,[28] facilitating visible light-mediated chemical photocatalysis through two-photon excitation within a singular catalytic cycle. The approach utilized a perylene bisimide (PDI) fluorescence dye molecule, triggering the formation of a colored radical anion upon exposure to blue light (455 nm) in the presence of the electron donor triethylamine (Et3N). This photoexcited radical anion ($PDI^{\bullet-}$) then acted as a reagent for the photoreduction of aryl halides.[3]

RESULTS AND DISCUSSIONS

We initiated our experimental investigation using 1-benzylquinoxalin-2(1H)-one as a model substrate to optimize the reaction condition for achieving regioselective C-3 oxygenation of quinoxalin-2(1H)-ones, as summarized in Table 1. Our initial attempt involved introducing 2 equiv of KO^tBu into a DMSO solvent and allowing the reaction to proceed for 4 h at room temperature under aerobic conditions. This initial effort resulted in a 56% yield of the desired product, quinoxaline-2,3-dione (**2a**) (entry 1). Subsequently, by extending the reaction time up to 12 h, a progressive improvement in the reaction yields became evident (entries 2-4). Notably, at a 12 h reaction time, the yield of **2a** was substantially improved, reaching 92% (entry 4). However, further extension of the reaction time to 16 h did not yield a significant increase in product formation (entry 5). In addition to investigating the impact of reaction time, we held the reaction duration at 12 h while exploring other critical reaction parameters. When

alternative solvents such as acetonitrile (ACN), 1,4-Dioxane, and DMF were employed, the resulting yields were comparatively lower (entries 6-8). Notably, when THF and 1,2-DCE were utilized as solvents, the starting material remained unreacted (entries 9-10). Further observations indicated that increasing the KO^{t}Bu loading to 1 or 1.5 equiv led to reduced yields of 50% and 53%, respectively (entries 11 and 12). However, a more substantial KO^{t}Bu loading of 3 equiv resulted in an 80% yield of **2a** (entry 13). We also explored the impact of alternative reagents, specifically KOH and Cs_2CO_3, on the reaction yield. Employing KOH resulted in no **2a** formation (entry 14) while using Cs_2CO_3 led to only trace amounts of **2a** (entry 15). Interestingly, conducting the reaction under an argon atmosphere significantly diminished the reaction yield, resulting in only a trace amount of product formation (entry 16). Consequently, based on these comprehensive experimental investigations, we determined the optimal reaction conditions to involve 2 equiv of KO^{t}Bu loading in a DMSO solvent at room temperature under aerobic conditions, with a reaction time of 12 h.

Table 1. Condition Optimization

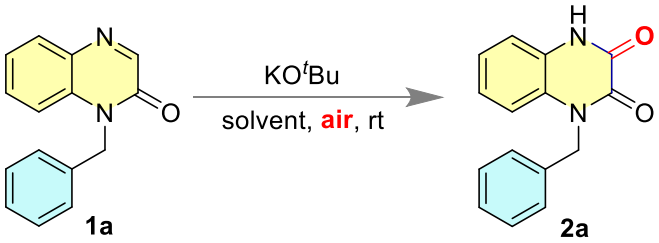

Entry	Reagent (equiv.)	Solvent	Time (h)	Yield (%)[b]
1	KO^{t}Bu (2.0)	DMSO	4	56
2	KO^{t}Bu (2.0)	DMSO	6	70
3	KO^{t}Bu (2.0)	DMSO	8	74
4	**KO^{t}Bu (2.0)**	**DMSO**	**12**	**92**
5	KO^{t}Bu (2.0)	DMSO	16	89

6	KO^{t}Bu (2.0)	ACN	12	61
7	KO^{t}Bu (2.0)	1,4-Dioxane	12	48
8	KO^{t}Bu (2.0)	DMF	12	34
9	KO^{t}Bu (2.0)	THF	12	NR[c]
10	KO^{t}Bu (2.0)	1,2-DCE	12	NR[c]
11	KO^{t}Bu (1.0)	DMSO	12	50
12	KO^{t}Bu (1.5)	DMSO	12	53
13	KO^{t}Bu (3.0)	DMSO	12	80
14	KOH (2.0)	DMSO	12	trace
15	Cs_2CO_3 (2.0)	DMSO	12	NR[c]
16	KO^{t}Bu (2.0)	DMSO	12	trace[d]

[a]Standard Conditions **1a** (0.169 mmol), KO^{t}Bu (2.0 equiv.) in 2 mL of solvent at room temperature for 12 h in aerobic condition.[b] Isolated Yield. [c]No Reaction. [d]Ar atmosphere.

Quinoxalin-2,3-dione is one of the important building blocks which are prevalent in bioactive molecules and natural products and is known to exhibit potential medicinal values. Their extensive applications are recognized in the diverse areas of industry and pharmacology.[29-30] We then broadened our exploration, using the optimized reaction conditions for this aerobic oxygenation process. We began by investigating various substituents at the N-1 position of quinoxalin-2(1H)-ones (Figure 2). Those with electron-donating groups like -^{t}Bu, -^{i}Pr, and -Me demonstrated successful involvement in the reaction, yielding products **2b** to **2d**, ranging from 77% to 89%. We also tested quinoxalin-2(1H)-ones with electron-withdrawing substituents like -CF_3, -F, 3,5-difluoro, and -Br at the N-1 position. Under the optimized conditions, these substrates delivered corresponding quinoxaline-2,3-diones **2e** to **2h**, with yields ranging from 82% to 87%. Extending our scope, we studied quinoxalin-2(1H)-ones containing diverse alkyl groups at the N-1 position, including -Et, -phenylethyl, and *n*-butyl.

These substrates smoothly transformed, producing desired products **2i** to **2k**, with yields between 72% and 85%. Impressively, even a quinoxalin-2(*1*H)-one with an alkynyl substitution at the N-1 position reacted favorably, yielding the corresponding product **2l** with a 70% yield. Additionally, we performed the reaction on a polyaromatic quinoxalin-2(1H)-one, yielding the desired product **2m** with an impressive 92% yield under standard conditions. Notably, the desired product was not obtained when an unsubstituted N-1 position of quinoxalin-2(1H)-one was employed as the substrate.

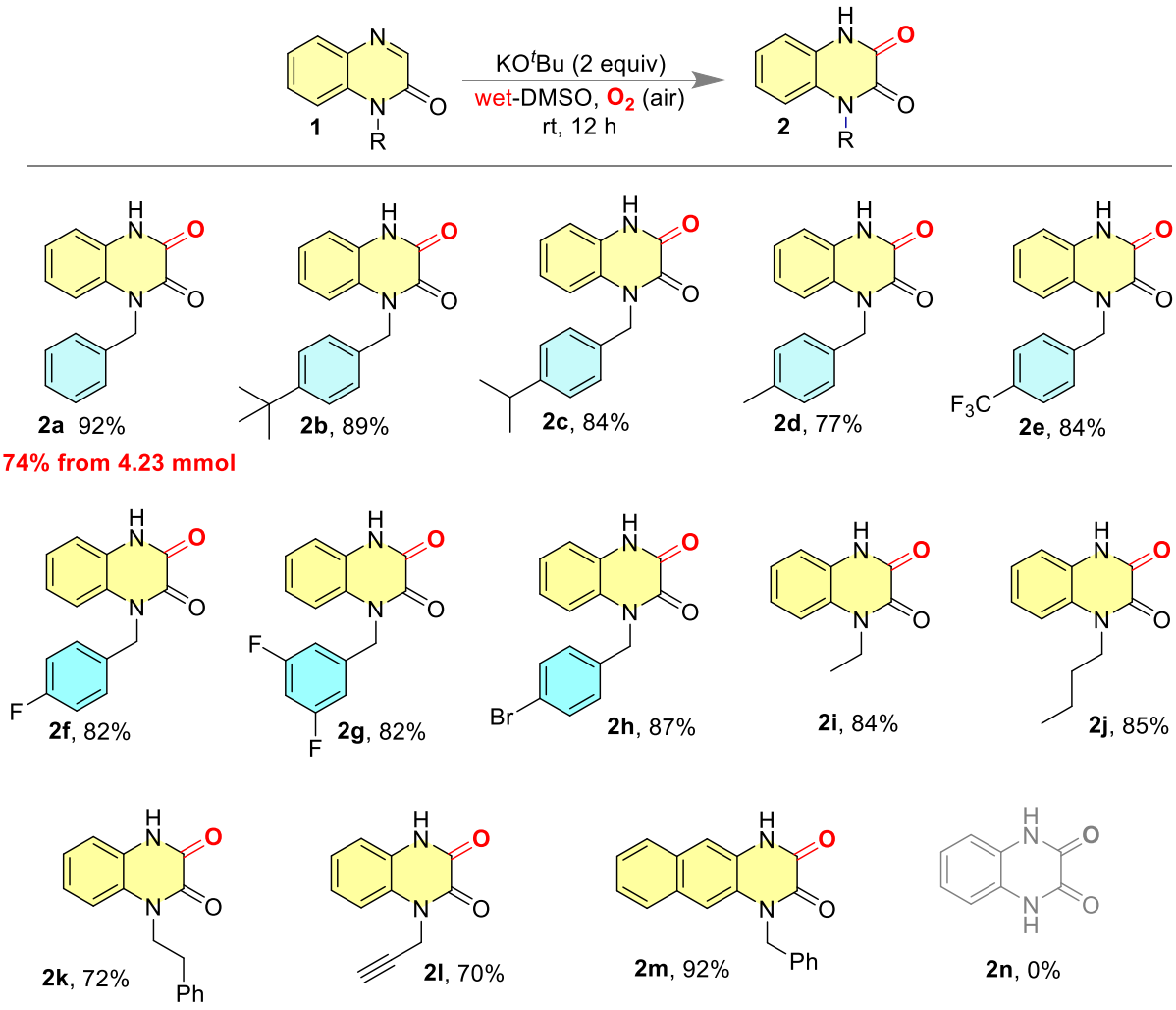

Figure 2. Scope of different substituents at *N*-1 position of quinoxalin-2(1*H*)-ones.

In addition, the substrate scope of the methodology was explored with variations in the *o*-phenylene diamine moiety (Figure 3). Quinoxalin-2(*1*H)-ones bearing disubstitutions on the o-

phenylene diamine part, featuring diverse electron-donating and electron-withdrawing groups, exhibited smooth reactivity, yielding **3a-3d** in 80-87% yields. For quinoxalin-2(*1*H)-ones with mono-substitution on the *o*-phenylene diamine portion, where the starting compounds were regioisomeric mixtures, different electron-donating or electron-withdrawing groups led to the formation of regioisomeric product mixtures **3e-3g**. A –Me substituent on the *o*-phenylene diamine part of the quinoxalin-2(*1*H)-one resulted in product **3e**, obtained in an 83% yield with a 5:3 regioisomeric ratio. Starting compounds monosubstituted with –Br and –Cl functionalities on the *o*-phenylene diamine fragment underwent conversion, yielding products **3f** and **3**g in 76% and 84% yields, respectively, with regioisomeric ratios of 2:1 and 3:1.

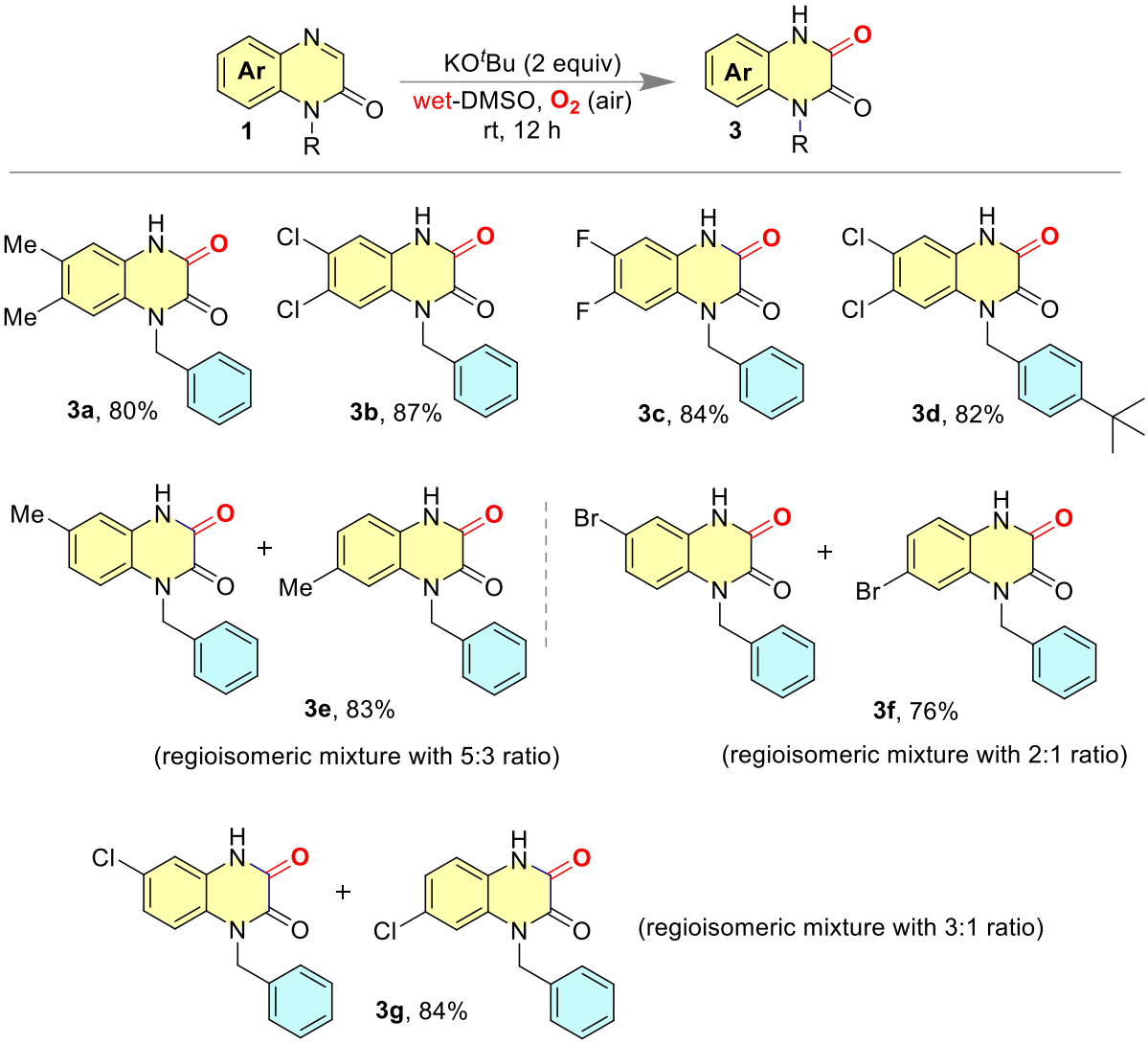

Figure 3. Substrates scope with different substituents in *o*-phenylenediamine part.

A series of control experiments were conducted to gain insights into the reaction mechanism (Figure 4). Figure 4a presents the outcomes when deviations from the standard conditions were examined. When the reaction was conducted under an argon atmosphere, a trace amount of product could be detected. Similarly, when the reaction was carried out in the absence of light, there was no significant change in the yield of **2a**. Furthermore, the reaction did not yield **2a** when KO*t*Bu was not used. These results indicate the critical roles played by aerial oxygen, KO^{t}Bu and the influence of light. The observations of the quenching experiments are shown in Figure 4b. The reaction produced compound **2a** with trace and 46% yields when conducted

using radical scavengers such as BHT (2,6-di-tert-butyl-4-methylphenol) and TEMPO (2,2,6,6-tetramethylpiperidin-1-yloxyl), respectively.[31] This outcome strongly suggests a radical pathway. The reaction was quenched in the presence of $CuCl_2$, which indicated the involvement of a single electron transfer (SET) pathway.[25] Furthermore, the reaction proceeded efficiently in the presence of a singlet oxygen quencher, sodium azide, that ruled out the contribution of singlet oxygen to the reaction.[25] Furthermore, when the reaction was conducted in dry DMSO solvent under an O_2 atmosphere, only a trace quantity of **2a** was obtained (Figure 4c). However, when the same conditions were applied with the presence of 1.2 equiv of H_2O, **2a** was isolated with an 85% yield of (Figure 4c) and also from the isotopic labelling experiment in presence of D_2O the deuterated quinoxalin-2,3-dione was formed, detected by HRMS analysis which further suggests the protonation occurs from water (Figure 4d). These control experiments strongly suggest the pivotal involvement of H_2O in the reaction mechanism, potentially facilitating the protonation of reaction intermediates (*vide infra*). To investigate whether the molecular oxygen is coming from air or not the isotopic labelling experiment was performed in presence of $H_2{}^{18}O$ and HRMS data revealed that there was no formation of ^{18}O incorporated quinoxalinone-2,3-dione product. This observation indicates that the oxygen source was the air (Figure 4d).

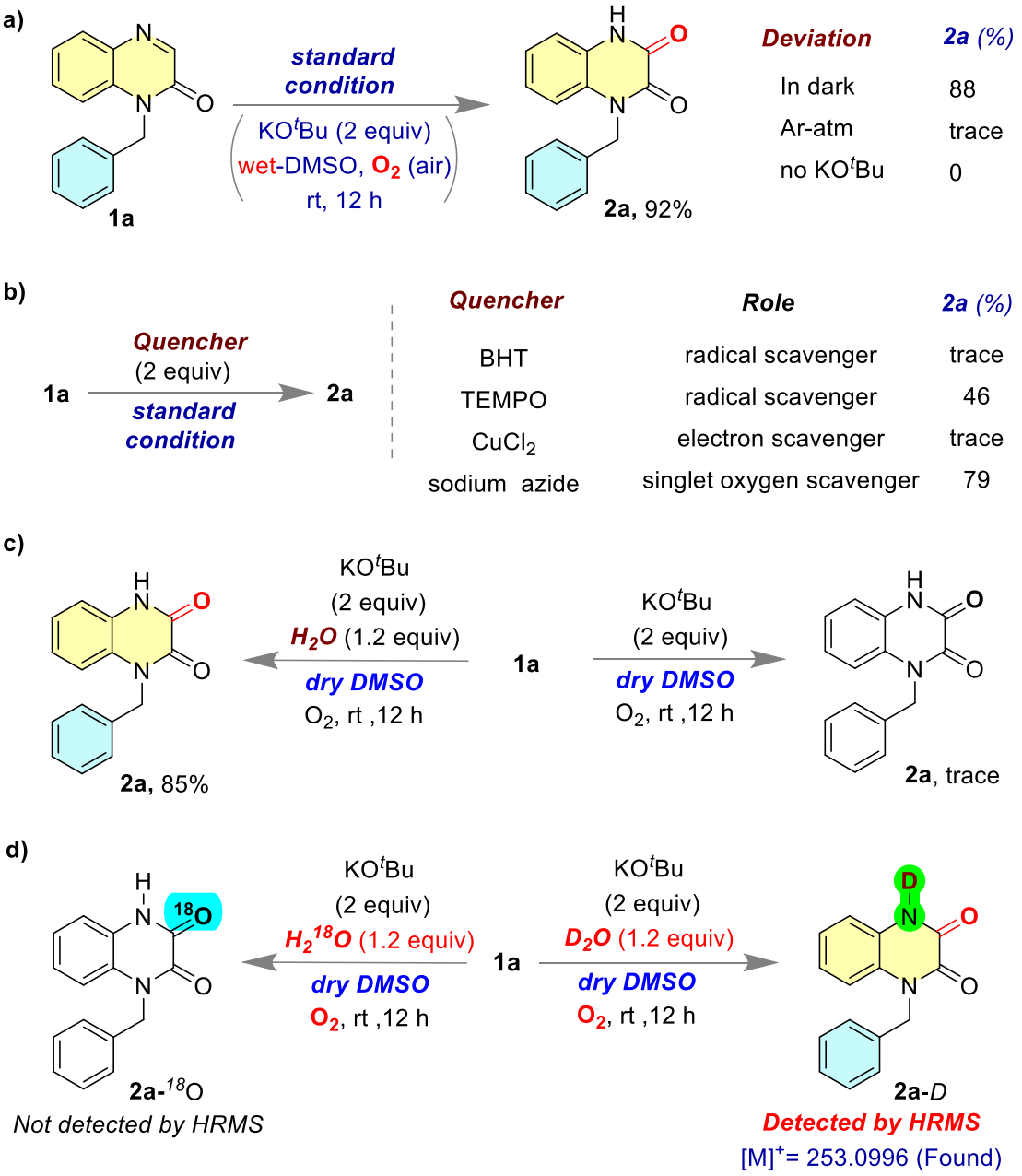

Figure 4. Control Experiments. a) Involving variation of reaction parameters. b) Incorporating various quenchers. c) Employing water in dry DMSO. d) Isotopic labelling experiments by D_2O and $H_2{}^{18}O$.

KO^{t}Bu is a colorless, white crystalline substance that does not absorb light. It is employed as an electron transfer reagent, while BHT serves as the radical trapping agent (Figure 5a). When a solution containing **1a** and potassium KO^{t}Bu in DMSO was prepared, a noticeable color change was observed, changing from colorless to purple (Figure 5a, right). In Figure 5b, the UV-Vis absorption spectra of **1a** and a series of mixtures are shown, including **1a** with KO^{t}Bu and **1a** with KO^{t}Bu in the presence of BHT. Upon addition of KO^{t}Bu to a solution of **1a** in DMSO, a bathochromic shift emerged at 429 nm, contrasting with the initial absorption at 347 nm. This shift likely arises due to the formation of a charge transfer complex between KO^{t}Bu and **1a**. Furthermore, the addition of BHT to the mixture of **1a** and KOtBu resulted in the appearance of a new absorption peak at 583 nm, which can be attributed to the generation of a stable radical anion of **1a**. This phenomenon occurs because BHT can be trapped by KO^{t}Bu, as depicted in Figure 5a, resulting in electron transfer to **1a**. Examining the UV-Vis spectrum of the solution containing **1a** and KO^{t}Bu in DMSO at various time intervals revealed that the formed radical anion remains stable for approximately 4-5 h (Figure S7, supporting information). Figure 5c shows a significant change in the redox potential of **1a**, both before and after the addition of KO^{t}Bu. Analysis of the cyclic voltammetry (CV) data revealed that the oxidation potential of KO^{t}Bu measured at +0.53 V (vs Ag/AgCl in DCM), and the reduction potential of **1a** was -1.79 V (vs Ag/AgCl in DCM), indicating that direct electron transfer from KO^{t}Bu to **1a** was not feasible. However, following the addition of KO^{t}Bu, the potential of **1a** experienced a shift to +1.08 V and +1.43 V. This shift provided further evidence for the formation of a charge transfer complex at the initial stage. Based on FT-IR analysis, we observed that in **1a** (highlighted in green), two frequencies at 3007 cm^{-1} and 2914 cm^{-1} corresponding to C-H stretching vibrations disappeared upon the addition of KO^{t}Bu. However, the C=O stretching frequency at 1643 cm^{-1} remained consistent in both cases (Figure 5d). This observation confirms that the formed radical anion is localized exclusively on the C=N double

bond of the heteroarene, rather than on the carbonyl group. This conclusion is further supported by NMR analysis (Figure 5e). Upon the addition of KO^{t}Bu, the ^{13}C NMR data for quinoxalin-2(*1*H)-ones revealed changes consistent with the formation of a radical anion intermediate (Figure 5e). Specifically, the chemical shift of the C^2-carbonyl carbon (C^2=O) and the C^3 carbon in **1a** shifted from 153.4 and 154.5 ppm to 149.9 and 156.7 ppm, respectively. This shift towards lower ppm values for C^2=O suggests a shielding effect, indicating that the π*-antibonding orbital of C^2=O may have stabilized the radical at C^3. Additionally, the stabilization of the anion at N^4 may have contributed to the deshielding of C^3. Furthermore, through ESI-MS analysis of the radical trapping experiment involving BHT (see supporting information), we verified the trapping of a *tert*-butoxyl radical by BHT. This result provides confirmation of the occurrence of a single electron transfer (SET) from KO^{t}Bu to **1a** (Figure S76, supporting information).

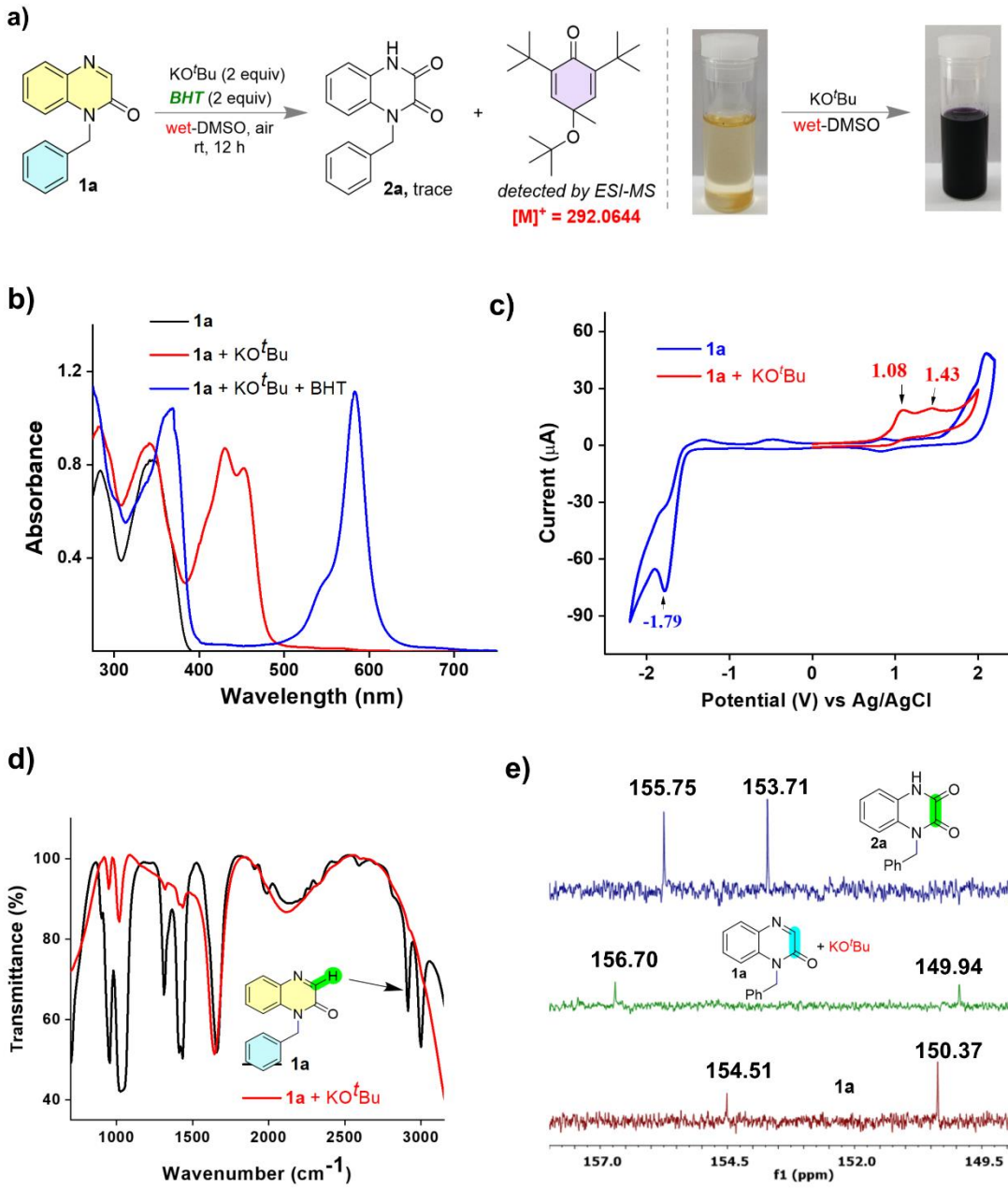

Figure 5. a) The reaction in the presence of BHT and the detection of BHT-adduct by ESI-MS (left) and the color change of **1a** in the presence of KO^{t}Bu in wet-DMSO. b) UV-Vis spectral change of **1a** and the mixture of **1a** with KO^{t}Bu (red) and **1a**, KO^{t}Bu with BHT (blue). c) Cyclic voltammogram of **1a** and **1a** with KO^{t}Bu. d) FT-IR analysis of **1a** and **1a** + KO^{t}Bu. e) Partial ^{13}C NMR spectra of **1a** (bottom), **1a** + KO^{t}Bu (middle) and **2a** (top) in DMSO-d_6.

The in-depth analysis derived from UV experiments, cyclic voltammetry studies, FT-IR spectral analysis, NMR spectroscopy, and ESI-MS data strongly indicates the likely formation of a stable radical anion intermediate preceding the oxygenation reaction. Drawing from both control experiments and existing literature evidence, a plausible mechanism is proposed in Figure 6.[21, 32] At first, KO^{t}Bu initiated the SET by donating an electron to compound **1**, forming the radical anion of quinoxalin-2(*1*H)-one. Subsequently, this radical anion activated dioxygen, giving rise to intermediate **I**.[31] Sequentially, intermediate **I** underwent a 1,3-hydrogen atom transfer (HAT), yielding intermediate **II**. Next, the peroxy bond in intermediate **II** experienced a homolytic cleavage, resulting in the formation of intermediate **III** along with H_2O_2.[33] Finally, intermediate **III** facilitated the formation of the desired product **2**.

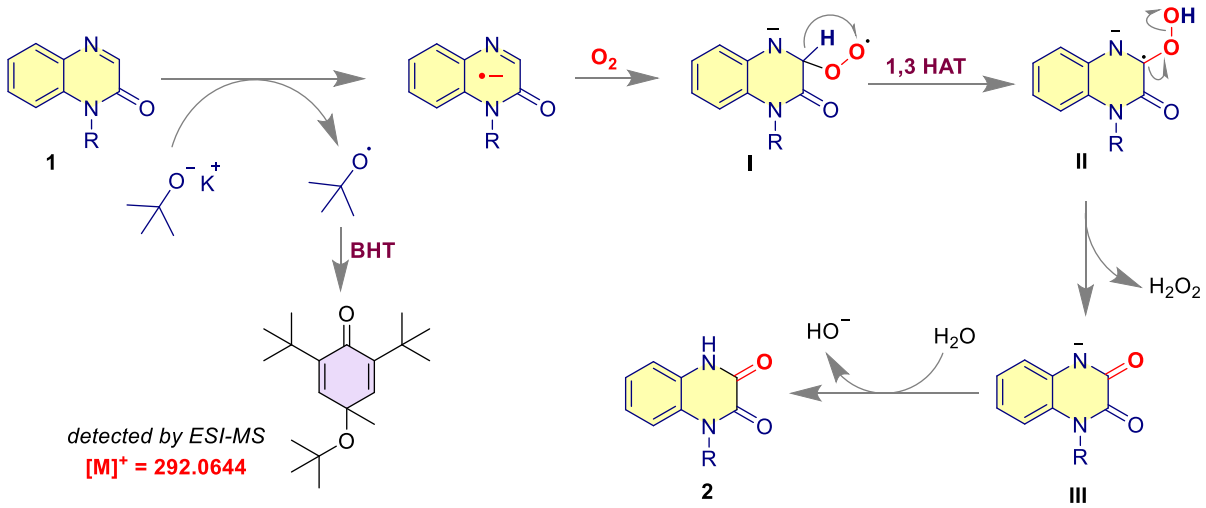

Figure 6. Plausible reaction mechanism for the conversion of **1** to **2**.

Remarkably, this study marks the first instance in the literature where a stable radical anion operates successfully in a moist atmosphere, enabling a chemical reaction involving atmospheric dioxygen activation. The mechanism involves the single electron transfer (SET) between KO^{t}Bu and quinoxalin-2(*1*H)-one, subsequently activating dioxygen to produce the

desired product. This straightforward method holds potential for applications in research domains like heterocycle synthesis and oxygenation chemistry.

CONCLUSION

In summary, this study demonstrates the activation of molecular dioxygen through the utilization of an in situ generated stable radical anion in a wet-condition. While radical anions show promise as visible light photocatalysts, challenges remain in creating stable variants due to their reactivity and susceptibility to environmental factors like air and moisture. This study represents the first documented instance in the literature of a stable radical anion functioning under an ambient atmosphere for a chemical reaction involving the activation of aerial dioxygen. The mechanism involves the single electron transfer (SET) between KO^{t}Bu and quinoxalin-2(*1*H)-one, followed by the activation of dioxygen, ultimately leading to the formation of the desired product. This straightforward procedure holds potential for diverse applications in research areas such as heterocycle synthesis and oxygenation chemistry.

ACKNOWLEDGMENT

Sudip Sau and Sathi Sahoo thank NISER for the fellowship. We are also thankful to Abhishek Raj and Uday Singh for their help during optimization studies.

REFERNCES

1. Y. Joo, V. Agarkar, S. H. Sung, B. M. Savoie and B. W. Boudouris, A nonconjugated radical polymer glass with high electrical conductivity, *Science*, 2018, **359**, 1391-1395. 10.1126/science.aao7287.
2. A. W. Misiołek, A. S. Ichimura, R. A. Gentner, R. H. Huang, V. P. McCaffrey and J. E. Jackson, Building Blocks for Molecule-Based Magnets: Radical Anions and Dianions of Substituted 3,6-Dimethylenecyclohexane-1,2,4,5-tetrones as

Paramagnetic Bridging Ligands, *Inorg. Chem.*, 2009, **48**, 9005-9017. 10.1021/ic901390n.

3. I. A. MacKenzie, L. Wang, N. P. R. Onuska, O. F. Williams, K. Begam, A. M. Moran, B. D. Dunietz and D. A. Nicewicz, Discovery and characterization of an acridine radical photoreductant, *Nature*, 2020, **580**, 76-80. 10.1038/s41586-020-2131-1.
4. J. Cann, B. S. Gelfand and G. C. Welch, Synthesis, self-assembly, and air-stable radical anions of unconventional 6,7-bis-nitrated N-annulated perylene diimides, *Molecular Systems Design & Engineering*, 2020, **5**, 1181-1185. 10.1039/D0ME00081G.
5. A. Studer and D. P. Curran, The Electron is a Catalyst, *Nat. Chem.*, 2014, **6**, 765-773. 10.1038/nchem.2031.
6. I. Ghosh, T. Ghosh, J. I. Bardagi and B. König, Reduction of aryl halides by consecutive visible light-induced electron transfer processes, *Science*, 2014, **346**, 725-728. 10.1126/science.1258232.
7. Y. Kumar, S. Kumar, K. Mandal and P. Mukhopadhyay, Isolation of Tetracyano-Naphthalenediimide and Its Stable Planar Radical Anion, *Angew. Chem., Int. Ed.*, 2018, **57**, 16318-16322. 10.1002/anie.201807836.
8. B. Tang, J. Zhao, J.-F. Xu and X. Zhang, Tuning the stability of organic radicals: from covalent approaches to non-covalent approaches, *Chem. Sci.*, 2020, **11**, 1192-1204. 10.1039/C9SC06143F.
9. H. Braunschweig, V. Dyakonov, J. O. C. Jimenez-Halla, K. Kraft, I. Krummenacher, K. Radacki, A. Sperlich and J. Wahler, An Isolable Radical Anion Based on the Borole Framework, *Angew. Chem. Int. Ed.*, 2012, **51**, 2977-2980. https://doi.org/10.1002/anie.201108632.
10. D. Bansal and P. Mukhopadhyay, Facile access to multi-state redox-active, push-pull naphthalenediimides: panchromatic radical anions and supramolecular networks, *J. Mater. Chem. C*, 2021, **9**, 3948-3956. 10.1039/d0tc05702a.
11. Y. Kumar, S. Kumar, D. Bansal and P. Mukhopadhyay, Synthesis and Isolation of a Stable Perylenediimide Radical Anion and Its Exceptionally Electron-Deficient Precursor, *Org. Lett.*, 2019, **21**, 2185-2188. 10.1021/acs.orglett.9b00490.
12. Z. X. Chen, Y. Li and F. Huang, Persistent and Stable Organic Radicals: Design, Synthesis, and Applications, *Chem*, 2021, **7**, 288-332. https://doi.org/10.1016/j.chempr.2020.09.024.

13. G. Sieg, I. Müller, K. Weißer and C. G. Werncke, Taming the stilbene radical anion, *Chem. Sci.*, 2022, **13**, 13872-13878. 10.1039/D2SC04451J.
14. D. B. G. Williams and M. Lawton, Drying of Organic Solvents: Quantitative Evaluation of the Efficiency of Several Desiccants, *J. Org. Chem.*, 2010, **75**, 8351-8354. 10.1021/jo101589h.
15. K. Fang, G. Li and Y. She, Metal-Free Aerobic Oxidation of Nitro-Substituted Alkylarenes to Carboxylic Acids or Benzyl Alcohols Promoted by NaOH, *J. Org. Chem.*, 2018, **83**, 8092-8103. 10.1021/acs.joc.8b00903.
16. L. Zhao, P. Yang, S. Shi, G. Zhu, X. Feng, W. Zheng, D. G. Vlachos and J. Xu, Activation of Molecular Oxygen for Alcohol Oxidation over Vanadium Carbon Catalysts Synthesized via the Heterogeneous Ligand Strategy, *ACS Catal.*, 2022, **12**, 15249-15258. 10.1021/acscatal.2c04601.
17. A. Bera, D. Sheet and T. K. Paine, Iron(ii)-α-keto acid complexes of tridentate ligands on gold nanoparticles: the effect of ligand geometry and immobilization on their dioxygen-dependent reactivity, *Dalton Trans.*, 2023, **52**, 1062-1073. 10.1039/D2DT02433K.
18. N. T. Vo, Y. Mekmouche, T. Tron, R. Guillot, F. Banse, Z. Halime, M. Sircoglou, W. Leibl and A. Aukauloo, A Reversible Electron Relay to Exclude Sacrificial Electron Donors in the Photocatalytic Oxygen Atom Transfer Reaction with O2 in Water, *Angew. Chem. Int. Ed.*, 2019, **58**, 16023-16027. https://doi.org/10.1002/anie.201907337.
19. E. Romero, J. R. Gómez Castellanos, G. Gadda, M. W. Fraaije and A. Mattevi, Same Substrate, Many Reactions: Oxygen Activation in Flavoenzymes, *Chem. Rev.*, 2018, **118**, 1742-1769. 10.1021/acs.chemrev.7b00650.
20. Y. Qian, D. Li, Y. Han and H.-L. Jiang, Photocatalytic Molecular Oxygen Activation by Regulating Excitonic Effects in Covalent Organic Frameworks, *J. Am. Chem. Soc.*, 2020, **142**, 20763-20771. 10.1021/jacs.0c09727.
21. J. P. Barham, G. Coulthard, K. J. Emery, E. Doni, F. Cumine, G. Nocera, M. P. John, L. E. A. Berlouis, T. McGuire, T. Tuttle and J. A. Murphy, KOtBu: A Privileged Reagent for Electron Transfer Reactions?, *J. Am. Chem. Soc.*, 2016, **138**, 7402-7410. 10.1021/jacs.6b03282.
22. X. Jin, K. Kataoka, T. Yatabe, K. Yamaguchi and N. Mizuno, Supported Gold Nanoparticles for Efficient α-Oxygenation of Secondary and Tertiary Amines into

Amides, *Angew. Chem. Int. Ed.*, 2016, **55**, 7212-7217. https://doi.org/10.1002/anie.201602695.

23. J. W. Kim, K. Yamaguchi and N. Mizuno, Heterogeneously Catalyzed Efficient Oxygenation of Primary Amines to Amides by a Supported Ruthenium Hydroxide Catalyst, *Angew. Chem. Int. Ed.*, 2008, **47**, 9249-9251. https://doi.org/10.1002/anie.200802464.
24. R. Ray, A. S. Hazari, S. Chandra, D. Maiti and G. K. Lahiri, Highly Selective Ruthenium-Catalyzed Direct Oxygenation of Amines to Amides, *Chem. Eur. J.*, 2018, **24**, 1067-1071. https://doi.org/10.1002/chem.201705601.
25. S. Sau and P. Mal, Visible-Light Promoted Regioselective Oxygenation of Quinoxalin-2(1H)-ones Using O_2 as an Oxidant, *J. Org. Chem.*, 2022, **87**, 14565-14579. 10.1021/acs.joc.2c01960.
26. W. Schilling, Y. Zhang, D. Riemer and S. Das, Visible-Light-Mediated Dearomatisation of Indoles and Pyrroles to Pharmaceuticals and Pesticides, *Chem. Eur. J.*, 2020, **26**, 390-395. https://doi.org/10.1002/chem.201904168.
27. H. Yi, C. Bian, X. Hu, L. Niu and A. Lei, Visible Light Mediated Efficient Oxidative Benzylic Sp3 C–H to Ketone Derivatives Obtained under Mild Conditions using O2, *Chem. Commun.*, 2015, **51**, 14046-14049. 10.1039/C5CC06015J.
28. Y. Sasaki, H. Kato and A. Kudo, [Co(bpy)3](3+/2+) and [Co(phen)3](3+/2+) electron mediators for overall water splitting under sunlight irradiation using Z-scheme photocatalyst system, *J. Am. Chem. Soc.*, 2013, **135**, 5441-5449. 10.1021/ja400238r.
29. D. Dewangan, K. Nakhate, A. Mishra, A. S. Thakur, H. Rajak, J. Dwivedi, S. Sharma and S. Paliwal, Design, Synthesis, and Characterization of Quinoxaline Derivatives as a Potent Antimicrobial Agent, *J. Heterocycl. Chem.*, 2019, **56**, 566-578. https://doi.org/10.1002/jhet.3431.
30. W. Xie, Y. Wu, J. Zhang, Q. Mei, Y. Zhang, N. Zhu, R. Liu and H. Zhang, Design, synthesis and biological evaluations of novel pyridone-thiazole hybrid molecules as antitumor agents, *Eur. J. Med. Chem.*, 2018, **145**, 35-40. https://doi.org/10.1016/j.ejmech.2017.12.038.
31. Y. Jin, L. Ou, H. Yang and H. Fu, Visible-Light-Mediated Aerobic Oxidation of N-Alkylpyridinium Salts under Organic Photocatalysis, *J. Am. Chem. Soc.*, 2017, **139**, 14237-14243. 10.1021/jacs.7b07883.

32. J. Madasu, S. Shinde, R. Das, S. Patel and A. Shard, Potassium tert-butoxide mediated C–C, C–N, C–O and C–S bond forming reactions, *Org. Biomol. Chem.*, 2020, **18**, 8346-8365. 10.1039/D0OB01382J.

33. I. Hermans, J. Peeters and P. A. Jacobs, Autoxidation of Ethylbenzene: The Mechanism Elucidated, *J. Org. Chem.*, 2007, **72**, 3057-3064. 10.1021/jo070040m.